Capillary Origami Inspired Fabrication of Complex 3D Hydrogel Constructs

Moxiao Li, Qingzhen Yang, Hao Liu, Mushu Qiu, Tian Jian Lu, and Feng Xu**

***H**ydrogels have found broad applications in various engineering and biomedical fields, where the shape and size of hydrogels can profoundly influence their functions. Although numerous methods have been developed to tailor 3D hydrogel structures, it is still challenging to fabricate complex 3D hydrogel constructs. Inspired by the capillary origami phenomenon where surface tension of a droplet on an elastic membrane can induce spontaneous folding of the membrane into 3D structures along with droplet evaporation, a facile strategy is established for the fabrication of complex 3D hydrogel constructs with programmable shapes and sizes by crosslinking hydrogels during the folding process. A mathematical model is further proposed to predict the temporal structure evolution of the folded 3D hydrogel constructs. Using this model, precise control is achieved over the 3D shapes (e.g., pyramid, pentahedron, and cube) and sizes (ranging from hundreds of micrometers to millimeters) through tuning membrane shape, dimensionless parameter of the process (elastocapillary number C_e), and evaporation time. This work would be favorable to multiple areas, such as flexible electronics, tissue regeneration, and drug delivery.*

1. Introduction

Hydrogels have found extensive applications in diverse engineering and biomedical territories, such as flexible electronics, tissue regeneration, and drug delivery.[1–6] Accumulating evidence has shown that the 3D shape and size of hydrogels are vital in these applications.[7–9] For example, alginate hydrogel spheres with a smaller diameter (300–500 μm) transplanted into mice elicited a severe fibrotic response, whereas those with a larger size (1.5–1.9 mm) did not elicit any severe fibrotic response.[10] Also, circular robs produced the minimal extent of foreign body response, compared to those of pentagonal and triangular geometries.[11] Microscale hydrogels, namely microgels, with specific 3D shapes have been used to mimic the functional units of different tissues (e.g., hexagonal liver lobules[12] and sinusoid-shaped hepatic sinusoids[13]), which can be further assembled to fabricate large cellular constructs.[14–16] Besides, disc-shaped microgels have been reported to possess a higher targeting efficiency than those having spherical geometry.[17] Hence, it is of great importance to fabricate 3D hydrogel constructs with controllable shape and size.

Numerous strategies have been developed to fabricate complex 3D hydrogel constructs, such as molding,[18–20] soft lithography,[21–23] two-photon lithography,[24–27] microfluidics,[28–32] and 3D printing.[31,33–35] Nevertheless, limitations are somewhat associated with existing scenarios.

M. Li, Prof. T. J. Lu
State Key Laboratory for Strength and Vibration of Mechanical Structures
School of Aerospace
Xi'an Jiaotong University
Xi'an 710049, P. R. China
E-mail: tjlu@mail.xjtu.edu.cn

M. Li, Dr. Q. Yang, H. Liu, M. Qiu, Prof. T. J. Lu, Prof. F. Xu
Bioinspired Engineering and Biomechanics Center (BEBC)
Xi'an Jiaotong University
Xi'an 710049, P. R. China
E-mail: fengxu@mail.xjtu.edu.cn

Dr. Q. Yang, H. Liu, M. Qiu, Prof. F. Xu
MOE Key Laboratory of Biomedical Information Engineering
School of Life Science and Technology
Xi'an Jiaotong University
Xi'an 710049, P. R. China

DOI: 10.1002/smll.201601147

For instance, the method of molding needs a specific mold for each geometrical structure, while soft lithography relies primarily on photopolymerization of liquid precursors, merely appropriate for photocrosslinkable hydrogels. Microfluidics usually employs specifically designed microchannels and multiphase systems to generate microparticles, requiring complex external devices or platforms (e.g., cleaning room or pumps) for such fabrication process.[28] Moreover, these approaches are not feasible for complex shapes, e.g., noncylindrical structures. Unfortunately, 3D printing, considered as a revolutionary method for fabricating complex 3D structures in a rapid, accurate, and high-throughput manner, is limited in printable hydrogel selection due to specific viscosity requirement of bioinks. Besides, the engagement of bulky and professional printing platform restricts its accessibility 3D printing. Therefore, there is still an unmet need for a facile, universal, yet widely accessible method to fabricate complex 3D hydrogel structures.

Recently, capillary force (i.e., surface tension) has been utilized to fold millimetric elastic membranes into 3D structures (termed as capillary origami).[36,37] The capillary force appears to be ideal for 3D mircofabrication since it becomes dominant at microscale compared with other forces such as gravitational or magnetic force. For instance, Py et al. found that depositing a water droplet on a thin flexible polydimethylsiloxane (PDMS) membrane can induce considerable membrane deformation due to capillary force; under specific conditions it could even lead to complete wrapping of the liquid with the evaporation.[36] Based on capillary origami, various 3D structures of the folded membrane have been constructed by deliberately designing the shape of the original flat membrane.[38–40] For such a phenomenon, no specific requirement is needed for the liquid, actually a variety of liquids (including water[36] and salt water[41]) have been used to generate the capillary force and fold elastic thin films in ≈10 min. However, these studies mainly focused on the final 3D structure of the membrane upon capillary origami closure. Hydrogel precursor, the prestate of hydrogel before crosslinking, can also be used to induce capillary forces.[42] Since it takes only tens of seconds to crosslink hydrogel with size varying from ≈100 µm to ≈1 mm, it is possible to freeze the 3D shape of hydrogel droplet at any time during the process of capillary origami. However, applying capillary origami to fabricate 3D hydrogel constructs is yet explored.

Making use of capillary origami, we developed a facile strategy to fabricate complex 3D hydrogel constructs with programmable shape and size. This method is simple and spontaneous, involving placing a hydrogel droplet on a PDMS membrane and subsequently crosslinking it at any moment during hydrogel evaporation. Further, we established a mathematical model to analyze the process, based on which we could achieve programmable shape and size of 3D hydrogel constructs. The developed method of fabricating hydrogel with complex 3D structures is broadly applicable for a wide range of hydrogels, holding great potential for broad applications such as tissue regeneration, drug delivery, and flexible electronics.

2. Theoretical Model

During spontaneous wrapping of a soft elastic membrane around a liquid droplet, the deformation of the membrane reduces the contact zone between liquid and air, hence decreasing the surface energy. The decreased surface energy (of order σL^2) is balanced by an increase in bending energy (of order B), so that the deformation occurs spontaneously when the surface energy overcomes the bending energy. The controllable variables of the fabrication process are Young's modulus of PDMS (E), membrane thickness (h), size of 2D pattern, and surface tension between liquid and air (σ). Considering the membrane as a thin elastic plate, we simplified the problem to a 2D case and ignored the gravity (Figure 2A). More specifically, a droplet with volume V is placed upon a thin solid membrane of total length L. The membrane may buckle under surface tension and hydrostatic pressure Δp. For a bent solid membrane, its deformation is governed by[43]

$$\frac{1}{\rho} = \frac{\mathrm{d}\theta}{\mathrm{d}s} = \frac{M}{EI} \tag{1}$$

where ρ is the radius of curvature, M is the bending momentum, I is the second momentum of area, θ is the angle between the membrane and horizontal line, and s is the arc length.

In the presence of surface tension and hydrostatic pressure, the bending moment can be expressed as

$$\begin{aligned} M(s) = {} & \sigma\cos\varphi_1(y_{\mathrm{end}} - y) + \sigma\sin\varphi_1(x_{\mathrm{end}} - x) \\ & - \frac{\sigma}{R}\int_s^{s_0/2}(y\sin\theta + x\cos\theta)\mathrm{d}s \\ & + y\frac{\sigma}{R}\int_s^{s_0/2}\sin\theta\,\mathrm{d}s + x\frac{\sigma}{R}\int_s^{s_0/2}\cos\theta\,\mathrm{d}s \end{aligned}$$

where φ_1 is the angle between the liquid droplet and the horizontal line as indicated in Figure 2A. Correspondingly, the boundary conditions can be written as

$$\begin{aligned} & \theta = 0 \quad \text{at } s = 0 \\ & \mathrm{d}\theta/\mathrm{d}s = 0 \quad \text{at } s = s_0/2 \end{aligned} \tag{2}$$

The profile of the membrane depends on the Young's modulus E, length/thickness of membrane and surface tension σ. The lengths (s, R, x, and y) are normalized by s_0, and V_0 by s_0^2. To integrate the parameters (E, σ, s_0, h) into one dimensionless parameter, elastocapillary number $C_e = \sqrt{\sigma s_0^2/EI} = \sqrt{12\sigma s_0^2/Eh^3}$ is introduced, which also manifests the importance of surface tension with respect to bending stiffness. The concrete solving process can be found in the Supporting Information.

3. Results and Discussion

The shape and size of hydrogels affect significantly their functions in their applications, which call for an effective method to fabricate complex 3D hydrogel constructs.

DOI: 10.1002/smll.201601147

Inspired by the phenomenon of capillary origami, we developed a facile method to fabricate complex 3D hydrogel constructs with programmable shapes and sizes by crosslinking versatile hydrogel droplets on thin PDMS membrane during arbitrary time point of the folding process (**Figure 1**). To fabricate the thin PDMS membrane, we developed a simple method by pipetting a certain volume of PDMS solution onto the surface of water (Figure S1, Supporting Information). The PDMS would spread out spontaneously upon the water and form a thin membrane. Upon curing, the membrane was transferred onto a polymethylmethacrylate (PMMA) substrate and cut into different shapes (regular triangle, trapezoid, cross, and four-angle star) and regular triangles with different side lengths (2, 3, and 5 mm). Various complex 3D hydrogel constructs were fabricated by crosslinking at any time point of the capillary origami folding process. The membrane wrapped on the hydrogel droplet can be easily peeled off due to hydrophobicity of the PDMS when shaking in water.

To control the fabrication process more efficiently, we established a mathematical model to predict the temporal evolution of 3D hydrogel structures during the process (**Figure 2**). Clearly, the fabrication of 3D structures from plain membranes depends largely on a combination of specific properties, including the Young's modulus (E), length/thickness of solid film (s_0, h), and surface tension (σ). A dimensionless elastocapillary number, C_e, is defined to compare the surface tension of the droplet with all the aforementioned properties of the membrane, so that the evolution of capillary origami would be discussed using C_e. During the bending process of elastic membrane, the normalized distance between two tips (L^*) is chosen to quantify its deformation for a given droplet volume V^* (Figure 2A).

To understand the regulatory mechanism of elastocapillary number for the whole process, we simulated the profile of droplet with decreasing liquid volume V^* and fixed C_e (i.e., mimicking the evaporation process), through which we obtained the change of L^* (representing the bending state of membrane) with decreasing V^* for selected values of C_e (Figure 2B). We observed two different modes, i.e., fully encapsulated and fold reopen, depending upon the value of selected C_e. When C_e is equal or bigger than 3.5 (e.g., $C_e = 3.5$ and $C_e = 4.0$), the distance L^* continuously decreases to zero with decreasing V^*, indicating that the membrane deforms continuously until completely wrapped, defined here as the fully encapsulate mode. Howbeit, when C_e is smaller than 3.5 (e.g., $C_e = 3.0$ and $C_e = 3.4$), the distance L^* decreases first and then increases with reducing V^*. The solid membrane, in such cases, folds up first and then reopens and hence is defined here as the fold-reopen mode. To validate the model, we performed experiments with PDMS membranes having different C_e values by tuning the thickness/side length of triangle PDMS membranes (Figure 2C). We observed that the fully encapsulated cases (Δ symbol) were below the solid line corresponding to $C_e = 3.5$, while the fold-reopen cases (o symbol) were above the line. The experimental results were consistent with the model prediction.

Based upon the prediction of our model, we fabricated 3D hydrogel structures with programmable shape and size by tuning the dimensionless parameter C_e and the droplet volume (i.e., evaporation time) (**Figure 3**). We observed that the membrane profile changes with evaporation time for all the cases studied. For example, at the very start, the profile is closer to the shape of spherical droplet. During evaporation, the volume of the droplet decreases and the capillary force gradually pulls the membrane, making the profile closer to the shape of deformed membrane. On the other hand, the deformation is dictated by the balance

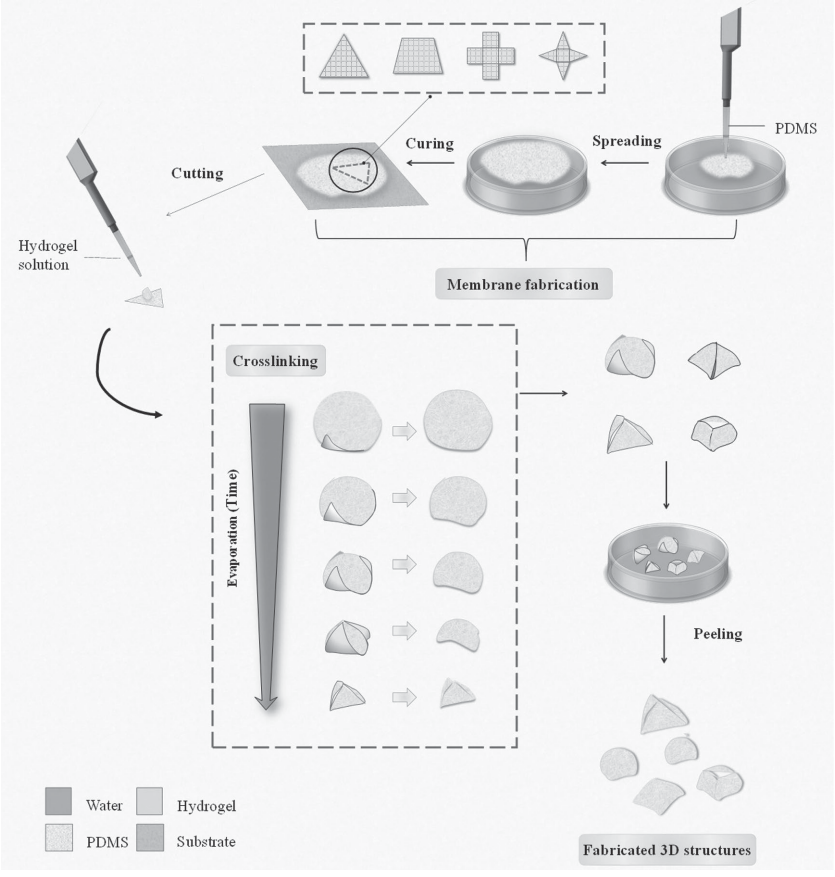

Figure 1. Schematic of capillary origami inspired fabrication of complex 3D hydrogel constructs. A thin PDMS membrane is fabricated by dripping a certain amount of PDMS solution onto the surface of water, which would spread out due to the surface tension of the water and the viscosity of the solution. After curing, the membrane is transferred to a PMMA substrate due to a stronger interaction and cut into different shapes and sizes as designed. A series of complex 3D hydrogel constructs can then be fabricated by crosslinking at any time point of the capillary origami folding process. The membrane wrapped on the hydrogel can be easily peeled off due to the hydrophobicity of the PDMS when shaking in water.

DOI: 10.1002/smll.201601147

www.MaterialsViews.com

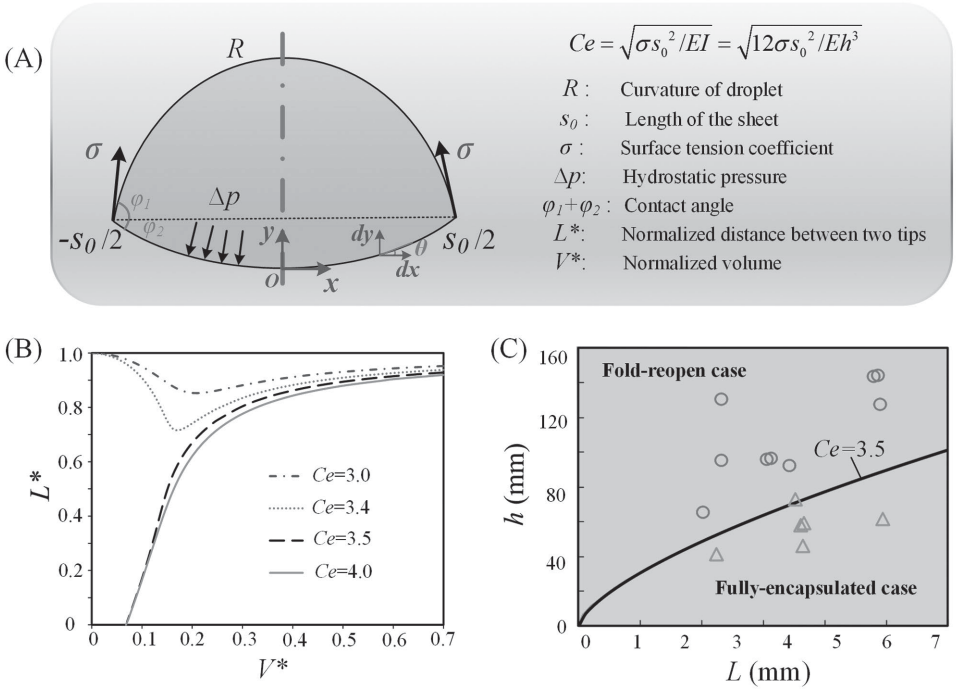

Figure 2. Mathematical modeling of the capillary origami. A) Geometry and coordinate system for a 2D capillary origami. B) The dimensionless distance between membrane tips L^* changes with the dimensionless volume V^* of droplet on the membrane under different elastocapillary numbers (C_e = 3.0, 3.4, 3.5, 4.0). C) Relationship between critical side length L and thickness h of a regular triangle membrane for folding. Points above the line (o) stand for experimental data of the fold-reopen case. Points below the line (Δ) stand for experimental data of fully encapsulated case.

of capillary force and bending stiffness of the membrane. As the value of C_e is changed, the profiles are different even if the droplet has the same droplet volume. Two different modes, the fold-open mode and fully encapsulated mode, can be converted to one another by tuning C_e. For relatively small elastocapillary number (e.g., C_e = 3.0, 3.4), the PDMS membrane folds up first and then reopens as the droplet volume decreases (i.e., fold-reopen mode) (Figure 3A,B). The membrane eventually becomes flat again when the liquid evaporates completely (V^* = 0). If C_e is greater than the critical value (3.5 in this study), the solid membrane would fold completely at the end (i.e., fully encapsulate mode) (Figure 3C,D). These results are consistent with the observation in experiments (Figure 2B).

The hydrogel structure's size and shape can be tuned by the membrane size and shape (**Figure 4**). We take the triangle PDMS membrane as a demo, the membranes having side lengths of 2, 3, and 5 mm are fabricated. To demonstrate this, we fabricated membranes with different 2D shapes (regular triangle, trapezoid, cross, and four angle star) and sizes (2, 3, and 5 mm). Taking these membranes, we crosslinked the hydrogels at closure of regular triangle PDMS membrane, through which we obtained pyramid-shaped hydrogels with different sizes (Figure 4A). This technique could be extended to wider range of scales. However, there are some hurdles that prevent the miniaturization (downsizing) and/or macro (upsizing). Theoretically, capillary force is proportional to the typical length of the structure L, while the elastic/pressure force is proportional to L^2 and the body force (e.g., gravity) is proportional to L^3.[44] The other forces decrease faster than capillary force when the sizes are scaled down. For instance, gravity effect becomes dominant in centimeter scale resulting in the flattening of the capillary origami structure. In order to get a steric structure, other forces need to be introduced into the system to balance the gravity under such circumstance. While for smaller scales (e.g., submillimeter), the relative ratio between thickness and length of the membrane increases, leading to hard deformation of the membrane. This situation, on the one hand, can be fixed by introducing other forces as well, contributing to the membrane folding or unfolding (e.g., adding MNPs into membrane and deform the membrane magnetically). On the other hand, a thinner membrane fabrication can be achieved by means of micro/nanotechniques, making it easier to deform the membrane by capillary force solely. The preparation of such tiny scale membrane remains a challenge, pending further discussion on the smallest critical dimension.

Besides pyramid-like hydrogels, other shaped hydrogels are also in need. This could be achieved by tailoring the geometry of the PDMS film. We fabricated a cross-shaped membrane, by which a cubic hydrogel was obtained via the capillary origami-based method (Figure 4B(iii)). Such a cubic hydrogel is widely used in tissue regeneration and may found plenty of applications.[45–47] Other shapes of the hydrogel could be obtained by carefully tailoring the geometry of the PDMS film (Figure 4B). For instance, pentahedron hydrogel was obtained from four-angle-star-shaped membrane (Figure 4B(iv)) and wedge-shaped hydrogel was successfully fabricated by isosceles triangle membrane.

DOI: 10.1002/smll.201601147

small NANO MICRO

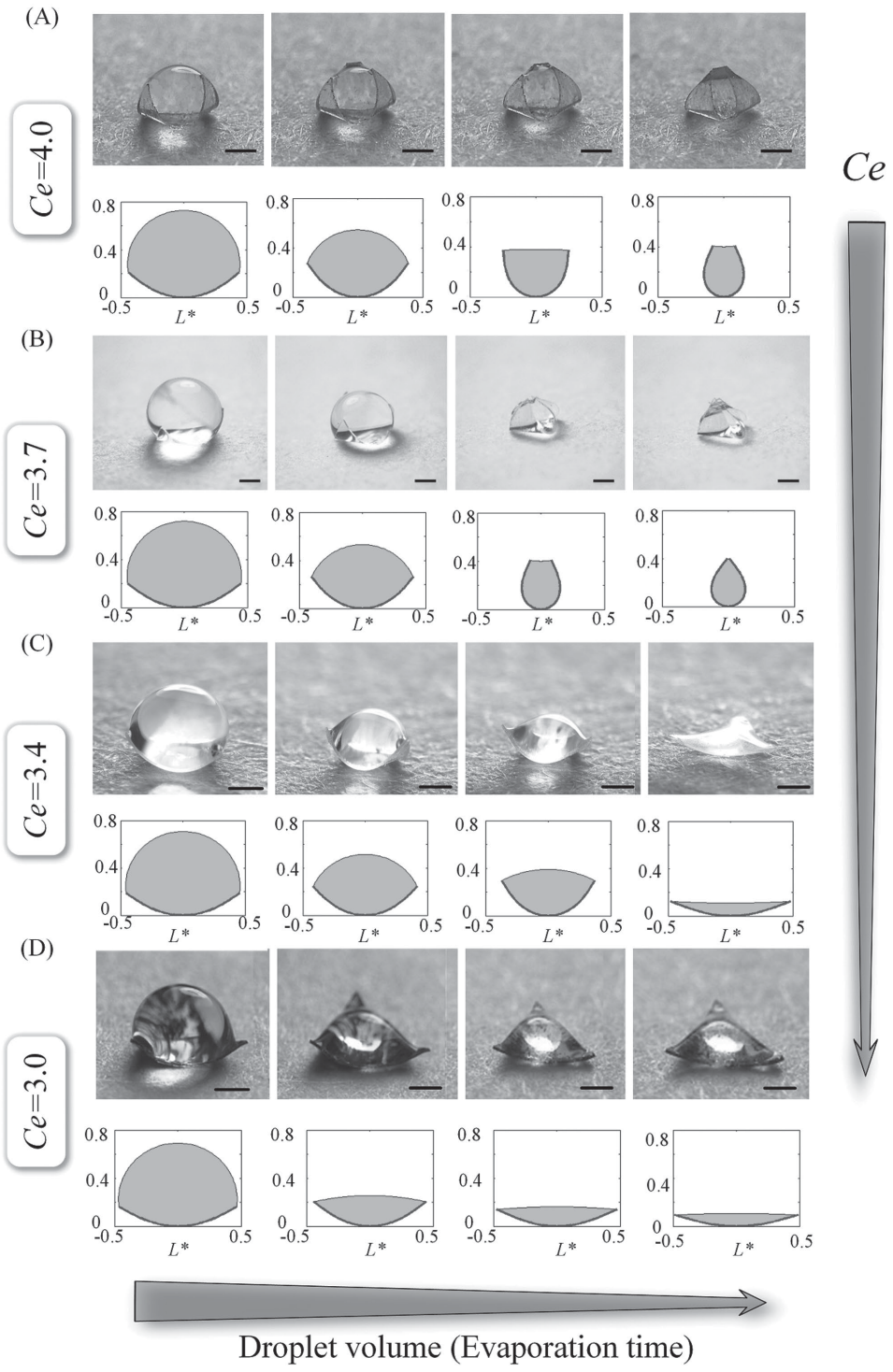

Figure 3. Fabrication of 3D hydrogel structures with programmable shapes and size through tuning the Elastocapillary numbers (C_e) and evaporation time. The evolution of capillary origami and the associated droplet profile compared with experimental images for C_e= A) 4.0, B) 3.7, C) 3.4, and D) 3.0. A,B) The membrane eventually comes into closure due to evaporation. C,D) The membrane bends with evaporation to some extend but not close and then return to the flat state (scale bar: 1 mm).

The final shape of hydrogel is quite stable after crosslinking the hydrogel and removing the PDMS membrane, and the surface tension will no longer play a part in deforming the structure when the hydrogel is completely crosslinked (Figure 4B). For those aforementioned membranes, we define them as deployable (i.e., the film can unfold to a flat membrane and also fold up into a 3D smooth structure). Other shaped membranes can also cause origami. For instance, Paulsen et al. used a rounded thin membrane and obtained an optimally efficient shape.[48] This is very similar to our method expect the optimally efficient structure is not smooth but with some ripples on its surface. This capillary

DOI: 10.1002/smll.201601147

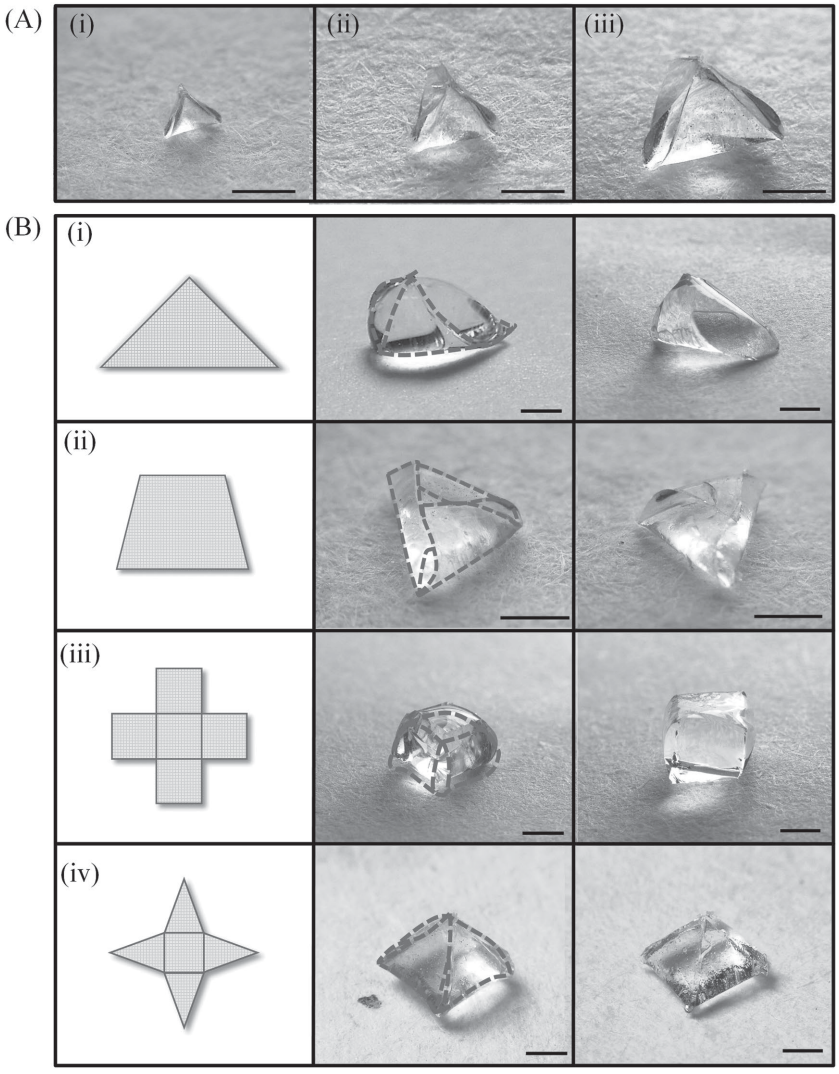

Figure 4. 3D hydrogel constructs fabricated with PDMS membranes of different sizes and shapes. A) 3D hydrogel constructs fabricated with PDMS membranes of different sizes. Length of the regular triangle PDMS membranes is (i) 2 mm, (ii) 3 mm, and (iii) 5 mm. B) 3D hydrogel constructs fabricated with PDMS membranes of different shapes: (i) isosceles triangle, (ii) trapezoid, (iii) cross, (iv) four angle star (scale bar: 1 mm).

origami-based method holds great potential in fabricating different shaped hydrogels as long the geometry of the membrane is well defined.

In our experiment, the initial concentration of polyethylene glycol (PEG) 1000 was 5 wt% and finally became 10–20 wt% due to evaporation. As the amount of the PEG molecular does not change during the evaporation, we can calculate the final concentration of the hydrogel according to the change of volume. We have fabricated 10 wt% concentration cylindrical hydrogel samples (diameter: 10 mm, height: 5 mm) by using two different approaches. One is the directly configured solution of 10 wt% concentration, and the other is prepared by enriching the solution of 5 wt% concentration to 10 wt% through evaporation. We measured their material mechanical property by indentation test (Figure S4, Supporting Information) and found no significant difference on Young's modulus of these samples fabricated from different approaches. Hence, the mechanical property can be predicted by regulating the initial concentration and the change of the liquid volume.

Moreover, our method can be combined with other techniques to significantly enhance the fabrication throughput capability. To demonstrate this, we combined our method with 3D printing to fabricate an array of hydrogels. A 5 × 5 array of regular triangle membranes were placed under 3D platform with nanoscale resolution and same volume of hydrogel precursor was injected onto the membrane (3 mm) (**Figure 5**A).

Versatile applications of hydrogels often require multiworking environment and thus need degradation under different physiological conditions. There is an urge demand of various kinds of hydrogel fabrication. Besides photosensitive hydrogel, our method is also compatible with other types of hydrogels, such as thermal crosslinkable hydrogel (GelMA) and chemical crosslinkable hydrogel (alginate) (Figure 5B(i) and (ii)). Photosensitive hydrogel (10 wt% PEG) with MNPs can also be fabricated and used for further self-assembly (Figure 5B). These materials have well-demonstrated good biocompatibility and have been widely used in many biomedical applications.[49,50] Furthermore, these hydrogels can be used to encapsulate various cells to generate cell-laden building blocks, holding great potential in bottom-up tissue engineering.

Practically, there are still lots of room for the development of our method. Since evaporation is not the only way to control the capillary origami process, other kinds of forces can additionally be adopted into the systems to coregulate the procedure of fabricating complex 3D constructs. As discussed above, field forces (e.g., electric force or magnetic force) can help to deform the membrane or balance the gravity in large scale. Such forces can be easily controlled by external physical field, making it possible to switch the fold and unfold cases at will. For example, based on electrowetting, an electric field was employed to acting against surface tension, promoting the reopening of the membrane.[41]

In addition, engaging advanced micro/nanotechniques will benefit the mass production of the eventual products. Fabricating hydrogels with submillimeter dimensions (i.e., microgels) would be more appealing in numerous biological applications. For this, micro/nanofabrication techniques (e.g., mold–demolding method) could help to produce a precisely designed mould, facilitating the construction of well-tailored PDMS membranes with smaller sizes. Moreover, with advanced fabrication method, delicate membranes with more complex shapes could be obtained, which can be used to fabricate complex hydrogel constructs. These multiple hydrogel

DOI: 10.1002/smll.201601147

small NANO MICRO

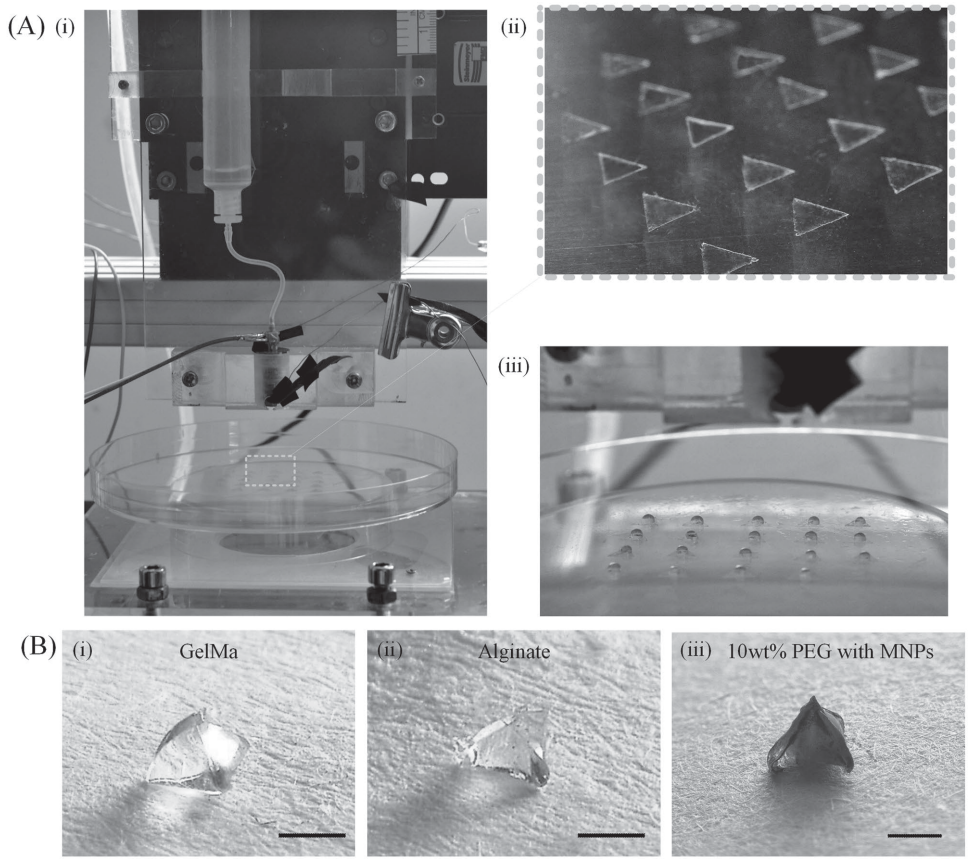

Figure 5. Throughput capability and compatibility with different types of hydrogels. A) Potential high-throughput fabrication of an array of hydrogels. (i) An array of membranes under 3D bioprinter. (ii) Magnified image of membranes. (iii) Printing droplets on membranes by 3D bioprinter. B) Different types of hydrogel including: (i) thermal crosslinkable hydrogel (GelMA), (ii) chemical crosslinkable hydrogel (alginate), and (iii) photosensitive hydrogel (10 wt% PEG) encapsulated with MNPs (scale bar: 1 mm).

units could be further assembled directly, presenting a facile strategy for future 3D tissue constructs.

4. Conclusion

In summary, we have developed a facile method for fabrication of complex 3D hydrogel constructs by using capillary force to fold and shape solid films and membranes, which would be difficult to obtain by other means. Built upon the capillary origami, well-controlled 3D hydrogel structures were produced by crosslinking during folding process. The profiles of the structure are dependent on crosslinking time, properties of the membrane and liquid, and the membrane shape. Moreover, the developed method holds great potential to be high throughput and applicable to a wide range of materials.

5. Experimental Section

Materials: Polydimethylsiloxane (PDMS) Sylgard 184 was obtained from Dow Corning, USA. PEG 1000 was purchased from Polysciences, Inc. Sodium alginate (LF20/40) was purchased from FMC Biopolymer. Gelatin-methacrylate (GelMA) and alginate were synthesized as previously described.[51,52] PMMA was purchased from Evonik Industries. PEG precursor was obtained by dissolving PEG and photoinitiator into water with concentration of 10 and 0.5 wt%, respectively. GelMA precursor was obtained by dissolving GelMA and the photoinitiator into water, with final concentrations of 5 and 0.3 wt%, respectively. Powder of alginate was dissolved in deionized water (content of alginate fixed at 15%) and a solution containing calcium chloride ($CaCl_2$, Sigma) was used to crosslink the alginate network.

Fabrication of PDMS Membrane: The PDMS membrane used in this study was fabricated by a simple and cost-effective method. Specifically, the PDMS monomers and curing agent were first mixed at the mass ratio of 10:1 and placed in vacuum to remove air bubbles for ≈30 min. Subsequently, upon pipetting the PDMS solution into a petri dish full of water, the PDMS solution spontaneously spread on the water surface. After 12 h, PDMS was cured in an oven for another 8 h at 40 °C, forming a thin PDMS membrane with a relatively uniform thickness. Due to the stronger interaction between PDMS and PMMA than that with water, the PDMS membrane was transferred to a PMMA substrate to water facilitates the peeling off of PDMS from the fabricated 3D hydrogel (Figure 1). The thickness of the PDMS membranes can be tuned by changing the PDMS volume and petri dish size (Figure S1, Supporting Information). In this way, PDMS membranes with different thicknesses (from ≈40 to ≈100 μm) were fabricated and manually cut into different 2D shapes (regular triangle, trapezoid, cross, and four-angle star) and sizes (e.g., side length of regular triangle

DOI: 10.1002/smll.201601147

varied as 2, 3, and 5 mm). The thickness h and the characteristic length s_0 of the elastic membrane were measured by an optical microscopy (KEYENCE VHX-600E). The Young's modulus E of the PDMS was measured by a nanoindentation machine in our lab. With these measurements, C_e can be calculated through equation $C_e = \sqrt{\sigma s_0^2/EI} = \sqrt{12\sigma s_0^2/EH^3}$.

Fabrication of 3D Hydrogel Structures: To fabricate 3D hydrogel structures, a droplet of PEG precursor solution mixed with photo initiator (final concentration of 10–20 and 0.5 wt%, respectively) was pipetted onto a regular triangle PDMS membrane. With evaporation at room temperature (25 °C), the surface tension of the droplet pulled the membrane and gradually deformed it. The hydrogel structures were frozen via UV radiation as its crosslinking time is much shorter than the closure time (Figure S2, Supporting Information). Each 3D hydrogel construct was imaged using an optical microscopy (KEYENCE VHX-600E), through which its shape and size were characterized.

Supporting Information

Supporting Information is available from the Wiley Online Library or from the author.

Acknowledgements

This work was financially supported by the National Natural Science Foundation of China (11372243, 11522219, 11532009) and the Fundamental Research Funds for the Central Universities (xjj2016074). Q.Y. also acknowledges the partial support from the China Postdoctoral Science Foundation (2015M570826), National Engineering Laboratory for Highway Maintenance Equipment (Chang'an University) (310825161103), and the Foundation of Shaanxi Postdoctoral Science.

[1] A. Jain, M. Betancur, G. D. Patel, C. M. Valmikinathan, V. J. Mukhatyar, A. Vakharia, S. B. Pai, B. Brahma, T. J. MacDonald, R. V. Bellamkonda, *Nat. Mater.* **2014**, *13*, 308.
[2] Y. S. Kim, M. Liu, Y. Ishida, Y. Ebina, M. Osada, T. Sasaki, T. Hikima, M. Takata, T. Aida, *Nat. Mater.* **2015**, *14*, 1002.
[3] S. Merino, C. Martín, K. Kostarelos, M. Prato, E. Vázquez, *ACS Nano* **2015**, *9*, 4686.
[4] J. Xu, S. Strandman, J. X. X. Zhu, J. Barralet, M. Cerruti, *Biomaterials* **2015**, *37*, 395.
[5] S. M. Saraiva, S. P. Miguel, M. P. Ribeiro, P. Coutinho, I. J. Correia, *RSC Adv.* **2015**, *5*, 63478.
[6] S. Lin, H. Yuk, T. Zhang, G. A. Parada, H. Koo, C. Yu, X. Zhao, *Adv. Mater.* **2016**, *28*, 4497.
[7] I. A. Eydelnant, B. Betty Li, A. R. Wheeler, *Nat. Commun.* **2014**, *5*, 3355.
[8] S. Muro, C. Garnacho, J. A. Champion, J. Leferovich, C. Gajewski, E. H. Schuchman, S. Mitragotri, V. R. Muzykantov, *Mol. Ther.* **2008**, *16*, 1450.
[9] K. J. Lee, J. Yoon, J. Lahann, *Curr. Opin. Colloid Interface Sci.* **2011**, *16*, 195.
[10] O. Veiseh, J. C. Doloff, M. Ma, A. J. Vegas, H. H. Tam, A. R. Bader, J. Li, E. Langan, J. Wyckoff, W. S. Loo, S. Jhunjhunwala, A. Chiu, S. Siebert, K. Tang, J. Hollister-Lock, S. Aresta-Dasilva, M. Bochenek, J. Mendoza-Elias, Y. Wang, M. Qi, D. M. Lavin, M. Chen, N. Dholakia, R. Thakrar, I. Lacik, G. C. Weir, J. Oberholzer, D. L. Greiner, R. Langer, D. G. Anderson, *Nat. Mater.* **2015**, *14*, 643.
[11] B. F. Matlaga, L. P. Yasenchak, T. N. Salthouse, *J. Biomed. Mater. Res.* **1976**, *10*, 391.
[12] C.-T. Ho, R.-Z. Lin, R.-J. Chen, C.-K. Chin, S.-E. Gong, H.-Y. Chang, H.-L. Peng, L. Hsu, T.-R. Yew, S.-F. Chang, C.-H. Liu, *Lab Chip* **2013**, *13*, 3578.
[13] R. S. McCuskey, *Liver* **2000**, *20*, 3.
[14] H. Y. Long, Y. Yanshen, L. Shaobao, W. Jinhui, C. Yongmei, L. Tian Jian, X. Feng, *Biofabrication* **2013**, *5*, 035004.
[15] F. Xu, T. D. Finley, M. Turkaydin, Y. Sung, U. A. Gurkan, A. S. Yavuz, R. O. Guldiken, U. Demirci, *Biomaterials* **2011**, *32*, 7847.
[16] F. Xu, C.-A. M. Wu, V. Rengarajan, T. D. Finley, H. O. Keles, Y. Sung, B. Li, U. A. Gurkan, U. Demirci, *Adv. Mater.* **2011**, *23*, 4254.
[17] S. Muro, C. Garnacho, J. A. Champion, J. Leferovich, C. Gajewski, E. H. Schuchman, S. Mitragotri, V. R. Muzykantov, *Mol. Ther.* **2008**, *16*, 1450.
[18] W. Bian, B. Liau, N. Badie, N. Bursac, *Nat. Protoc.* **2009**, *4*, 1522.
[19] P. Occhetta, N. Sadr, F. Piraino, A. Redaelli, M. Moretti, M. Rasponi, *Biofabrication* **2013**, *5*, 035002.
[20] K. R. Stevens, M. D. Ungrin, R. E. Schwartz, S. Ng, B. Carvalho, K. S. Christine, R. R. Chaturvedi, C. Y. Li, P. W. Zandstra, C. S. Chen, S. N. Bhatia, *Nat. Commun.* **2013**, *4*, 1847.
[21] C. Moraes, J. M. Labuz, Y. Shao, J. Fu, S. Takayama, *Lab Chip* **2015**, *15*, 3760.
[22] J. Pan, S. Y. Chan, J. E. A. Common, S. Amini, A. Miserez, E. B. Lane, L. Kang, *J. Biomed. Mater. Res., Part A* **2013**, *101*, 3159.
[23] D. Qin, Y. Xia, G. M. Whitesides, *Nat. Protoc.* **2010**, *5*, 491.
[24] B. Kaehr, J. B. Shear, *Proc. Natl. Acad. Sci. USA* **2008**, *105*, 8850.
[25] J. Xing, J. Liu, T. Zhang, L. Zhang, M. Zheng, X. Duan, *J. Mater. Chem. B* **2014**, *2*, 4318.
[26] J. Xing, L. Liu, X. Song, Y. Zhao, L. Zhang, X. Dong, F. Jin, M. Zheng, X. Duan, *J. Mater. Chem. B* **2015**, *3*, 8486.
[27] Z. Xiong, M.-L. Zheng, X.-Z. Dong, W.-Q. Chen, F. Jin, Z.-S. Zhao, X.-M. Duan, *Soft Matter* **2011**, *7*, 10353.
[28] D. J. Beebe, J. S. Moore, J. M. Bauer, Q. Yu, R. H. Liu, C. Devadoss, B.-H. Jo, *Nature* **2000**, *404*, 588.
[29] S. Ma, J. Thiele, X. Liu, Y. Bai, C. Abell, W. T. Huck, *Small* **2012**, *8*, 2356.
[30] T. Odera, H. Hirama, J. Kuroda, H. Moriguchi, T. Torii, *Microfluid. Nanofluid.* **2014**, *17*, 469.
[31] J.-F. Xing, M.-L. Zheng, X.-M. Duan, *Chem. Soc. Rev.* **2015**, *44*, 5031.
[32] S. Allazetta, T. C. Hausherr, M. P. Lutolf, *Biomacromolecules* **2013**, *14*, 1122.
[33] C. B. Highley, C. B. Rodell, J. A. Burdick, *Adv. Mater.* **2015**, *27*, 5075.
[34] S. Hong, D. Sycks, H. F. Chan, S. Lin, G. P. Lopez, F. Guilak, K. W. Leong, X. Zhao, *Adv. Mater.* **2015**, *27*, 4035.
[35] A. L. Rutz, K. E. Hyland, A. E. Jakus, W. R. Burghardt, R. N. Shah, *Adv. Mater.* **2015**, *27*, 1607.
[36] C. Py, P. Reverdy, L. Doppler, J. Bico, B. Roman, C. N. Baroud, *Phys. Rev. Lett.* **2007**, *98*, 156103.
[37] S. Manakasettharn, J. A. Taylor, T. Krupenkin, in *Encyclopedia of Nanotechnology* (Ed: B. Bhushan), Springer,Netherlands **2012**, p. 383.
[38] S. Manakasettharn, J. A. Taylor, T. N. Krupenkin, *Appl. Phys. Lett.* **2011**, *99*, 144102.
[39] J. W. van Honschoten, J. W. Berenschot, T. Ondarçuhu, R. G. P. Sanders, J. Sundaram, M. Elwenspoek, N. R. Tas, *Appl. Phys. Lett.* **2010**, *97*, 014103.
[40] A. Antkowiak, B. Audoly, C. Josserand, S. Neukirch, M. Rivetti, *Proc. Natl. Acad. Sci. USA* **2011**, *108*, 10400.
[41] M. Pineirua, J. Bico, B. Roman, *Soft Matter* **2010**, *6*, 4491.

DOI: 10.1002/smll.201601147

[42] R. D. Schulman, K. Dalnoki-Veress, *Phys. Rev. Lett.* **2015**, *115*, 206101.
[43] Y.-C. Fung, *Foundations of Solid Mechanics*, Prentice Hall, Englewood Cliffs **1965**.
[44] B. Roman, J. Bico, *J. Phys.: Condens. Matter* **2010**, *22*, 493101.
[45] W.-G. Koh, A. Revzin, M. V. Pishko, *Langmuir* **2002**, *18*, 2459.
[46] A. S. Hoffman, *Adv. Drug Delivery Rev.* **2012**, *64*, 18.
[47] S. E. A. Gratton, P. A. Ropp, P. D. Pohlhaus, J. C. Luft, V. J. Madden, M. E. Napier, J. M. DeSimone, *Proc. Natl. Acad. Sci. USA* **2008**, *105*, 11613.
[48] J. D. Paulsen, V. Demery, C. D. Santangelo, T. P. Russell, B. Davidovitch, N. Menon, *Nat. Mater.* **2015**, *14*, 1206.
[49] N. A. Peppas, J. Z. Hilt, A. Khademhosseini, R. Langer, *Adv. Mater.* **2006**, *18*, 1345.
[50] J. W. Nichol, S. T. Koshy, H. Bae, C. M. Hwang, S. Yamanlar, A. Khademhosseini, *Biomaterials* **2010**, *31*, 5536.
[51] Y. Li, G. Huang, B. Gao, M. Li, G. M. Genin, T. J. Lu, F. Xu, *NPG Asia Mater.* **2016**, *8*, e238.
[52] J.-Y. Sun, X. Zhao, W. R. K. Illeperuma, O. Chaudhuri, K. H. Oh, D. J. Mooney, J. J. Vlassak, Z. Suo, *Nature* **2012**, *489*, 133.

Received: April 4, 2016
Revised: June 12, 2016
Published online: